ESAIM: PROCEEDINGS, December 2012, Vol. 38, p. 36-53
F. Coquel, M. Gutnic, P. Helluy, F. Lagoutière, C. Rohde, N. Seguin, Editors

MODELLING AND SIMULATION OF 2D STOKESIAN SQUIRMERS *

Nina Aguillon[1], Astrid Decoene[1], Benoît Fabrèges[1], Bertrand Maury[1] and Benoît Semin[2]

Abstract. Direct numerical simulations of the individual and collective dynamics of neutral squirmers are presented. "Squirmer" refers to a class of swimmers driven by prescribed tangential deformations at their surface, and "neutral" means that the swimmer does not apply a force dipole on the fluid. The squirmer model is used in this article to describe self-propelled liquid droplets. Each swimmer is a fluid sphere in Stokes flow without radial velocity and with a prescribed tangential velocity, which is constant in time in the swimmer frame. The interaction between two or more swimmers is taken into account through the relaxation of their translational and angular velocities. The algorithm presented for solving the fluid flow and the motion of the liquid particles is based on a variational formulation written on the whole domain (including the external fluid and the liquid particles) and on a fictitious domain approach. The constraint on the tangential velocity of swimmers can be enforced using two different methods: penalty approach of the strain rate tensor on the particles domain, or a saddle-point formulation involving a Lagrange multiplier associated to the constraint. This leads to a minimization problem over unconstrained functional spaces that can be implemented straightforwardly in a finite-element multi-purpose solver. In order to ensure robustness, a projection algorithm is used to deal with contacts between particles. Two-dimensional numerical simulations implemented with FreeFem++ are presented.

1. Introduction

An important feature of many micro-organisms is their ability to swim, which leads to emergent behaviours, such as collective motions [4, 19, 22] or macroscopic viscosity modification [32]. To analyse the basic physical mechanisms of these collective phenomena, we consider a simple model of swimming micro-organism, assumed to propel itself by generating tangential velocities on its surface without changing shape. This model, referred to as *squirmer*, was first introduced by Lighthill [23] and Blake [2] as an idealisation of spherical micro-organisms, such as *Opalina*. These micro-organisms move using appendages called cilia, which are small compared to their diameter and cover the whole surface. It is well known that, in order to allow for a net forward displacement in viscous flow, the movement of these cilia must be periodic but non-symmetric in time, as stated by the so-called scallop theorem of E. M. Purcell [29]. The squirmer model has recently been applied to colonies of flagellates, such as the green alga *Volvox* (see for instance [17] and [7]). It is also well-adapted to describe recently developed artificial swimmers which consist of self-propelled liquid droplets [34]. The continuous phase contains surfactant molecules, which are adsorbed at the droplet interface and react with a chemical contained in the droplet. In the experiments, the concentration profile of the surfactant at the interface becomes unstable,

* *This work has been supported by the ANR project MOSICOB "Modélisation et Simulation de Fluides Complexes Biomimétiques".*

[1] Université Paris-Sud 11, Département de Mathématiques, Bâtiment 425, 91405 Orsay cedex (France)

[2] Max-Planck Institut für Dynamik und Selbstorganisation, Am Fassberg 17, 37077 Göttingen (Germany)

and the droplet propels itself due to Marangoni stresses. Squirming motion is particularly appealing for the study of the hydrodynamics of micro-scale swimming, since the velocities in the near and far field around an isolated swimming organism are well-defined and can be described analytically (see for instance [17]).

We consider a simplified swimmer where the tangential motion is independent of time in its frame of reference, like in [16]. In the case of micro-organisms, this corresponds to a velocity field averaged on a time-scale which is larger than the beating period of the cilia [28]. In this paper, we only consider neutral swimmers, i.e. swimmers which do not apply a force dipole on the fluid and are therefore neither pullers nor pushers [6,24]. Furthermore, the swimmers are not subjected to any external force or torque, which means in particular that they are neutrally buoyant and non-bottom-heavy. We neglect the effect of tumbling and rotary diffusion.

We aim at reproducing individual and collective phenomena of dense suspensions of squirmers, by means of direct numerical simulations, which is the only available tool in this concentration range. Swimmers are modelled as circular bodies of constant radius, with a squirming velocity field prescribed on the surface. This velocity is time-independent, axisymmetric and tangential in the droplet frame. The axis of symmetry is the swimming direction when isolated in an unbounded still fluid. Since we are interested in modelling micro-droplets or micro-organisms that live in flows at low Reynolds number, we consider Stokes flows. The model leads to a coupled problem composed by the Stokes equations in the whole domain with particular boundary conditions on the particle boundaries, and the equilibrium of forces on each particle. We propose two methods to solve this problem in a fully coupled way. They are based on a variational formulation on the whole domain, including external fluid and particles. The squirmer motion constraint is enforced using either a penalty method or a Lagrange multiplier approach, while incompressibility is treated by duality. This leads to a minimization problem over unconstrained functional spaces which can be implemented straightforwardly in a finite-element multi-purpose solver like FreeFem++ [13]. In order to ensure robustness, an efficient algorithm is used to deal with contacts between particles.

Simulations are presented of dilute to concentrated suspensions of neutral squirmers, and the effective shear viscosity is computed in the case of sheared flow.

2. The model

We consider a connected bounded and regular domain $\Omega \subset \mathbb{R}^2$ and we denote by $(B_i)_{i=1,\dots,N}$ the swimming bodies, strongly included in Ω (see Fig 1 right). B denotes the domain occupied by the swimmers: $B = \cup_i B_i$. The domain $\Omega \setminus \bar{B}$ is filled with Newtonian fluid governed by the Stokes equations. Here, μ is the viscosity of the fluid. Since we consider a Newtonian fluid, the stress tensor σ writes

$$\boldsymbol{\sigma}(\mathbf{u}) = 2\mu\mathbb{D}(\mathbf{u}) - p\,\mathbb{I}, \quad \text{where} \quad \mathbb{D}(\mathbf{u}) = \frac{\nabla\mathbf{u} + (\nabla\mathbf{u})^T}{2}.$$

For the sake of simplicity in the description of this model, we will consider homogeneous Dirichlet conditions on $\partial\Omega$, although in our simulations we also prescribe periodic and biperiodic conditions. On the other hand, viscosity imposes a no-slip condition on the boundary ∂B of the rigid domain.

Swimmers are modelled as circular bodies of constant radius R_b, with a prescribed time-independent and axisymmetric tangential velocity field $\mathbf{u}_\theta$ in the frame of reference of the swimmer, that can be defined as follows in polar coordinates:

$$\mathbf{u}_\theta(\phi) \;=\; \alpha\,\sin(\phi-\theta)\,\mathbf{e}_\phi\,, \tag{1}$$

where ϕ denotes the polar coordinate and $\mathbf{e}_\phi$ the unit vector tangential to the surface. The parameters α is a constant value characterizing the individual swimming velocity of the squirmer, and θ defines its swimming direction. This squirming velocity field is illustrated on the left on Fig 1.

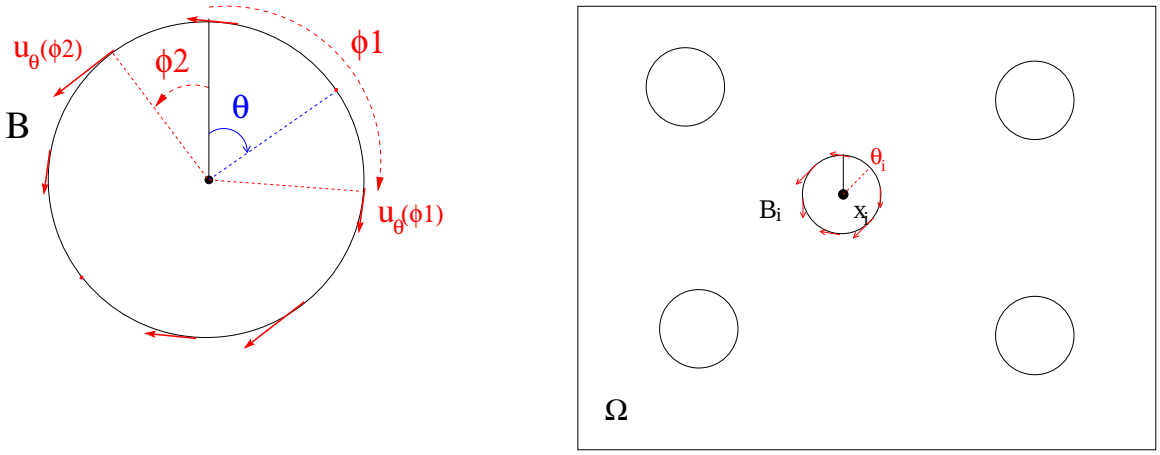

FIGURE 1. Left: Single squirmer and tangential velocity in the swimmers frame. Right: domain with inclusions

At the initial time the particles are distributed randomly over the fluid, without overlapping and with random swimming orientations. The position of the center of the ith swimming body is denoted by $\mathbf{x}_i$, its orientation angle by θ_i, and by $\mathbf{v}_i$ and ω_i its translational and angular velocities.

We have to find the velocity $\mathbf{u} = (u_1, u_2)$ and the pressure field p defined in $\Omega \setminus \bar{B}$, as well as the velocities of the swimmers $\mathbf{V} := (\mathbf{v}_i)_{i=1,...,N} \in \mathbb{R}^{2N}$ and $\boldsymbol{\omega} := (\omega_i)_{i=1,...,N} \in \mathbb{R}^N$ such that:

$$\left\{\begin{array}{rcll} -\mu\Delta\mathbf{u} + \nabla p &=& 0 & \text{in} \quad \Omega \setminus \bar{B}, \\ \nabla \cdot \mathbf{u} &=& 0 & \text{in} \quad \Omega \setminus \bar{B}, \\ \mathbf{u} &=& 0 & \text{on} \quad \partial\Omega, \\ \mathbf{u} &=& \mathbf{u}_{\theta_i} + \mathbf{v}_i + \omega_i \times (\mathbf{x} - \mathbf{x}_i) & \text{on} \quad \partial B_i, \quad \forall i \in \{1, ..., N\}. \end{array}\right. \tag{2}$$

No external force or couple is considered on the fluid nor on the swimmers, so that Newton's laws of motion, written here in the non-inertial regime, writes:

$$\left\{\begin{array}{rcl} \displaystyle\int_{\partial B_i} \sigma(\mathbf{u}) \cdot \mathbf{n} &=& 0 \quad \forall i, \\ \displaystyle\int_{\partial B_i} (\mathbf{x} - \mathbf{x}_i) \times \sigma(\mathbf{u}) \cdot \mathbf{n} &=& 0 \quad \forall i. \end{array}\right. \tag{3}$$

The motion of each swimmer is then set by its instantaneous velocity $\mathbf{u}(\mathbf{x}, t)$ defined on ∂B_i. More precisely, the individual translational velocity is equal to the average velocity:

$$\mathbf{v}_i(t) = \frac{1}{|\partial B_i|} \int_{\partial B_i} (\mathbf{u}(\mathbf{x}, t) - \mathbf{u}_{\theta_i}(\mathbf{x}, t)) \, , \tag{4}$$

and the individual angular velocity is equal to

$$\omega_i(t) = \frac{1}{|\partial B_i| \, |\mathbf{r}_i|^2} \int_{\partial B_i} (\mathbf{u}(\mathbf{x}, t) - \mathbf{u}_{\theta_i}(\mathbf{x}, t)) \times \mathbf{r}_i \, . \tag{5}$$

The swimmers dynamics are then set by the differential equations:

$$\dot{\mathbf{x}}_i(t) = \mathbf{v}_i(t) \, , \qquad \dot{\theta}_i(t) = \omega_i(t). \tag{6}$$

These differential equations introduce a dependency in time into the problem: Stokes equations are steady, but their solution depends on time because the configuration of the swimmers inside the fluid varies in time. Initial conditions must be associated to these differential equations. We will use random values for the initial data $\mathbf{x}_i(t=0)$ and $\theta_i(t=0)$.

3. Variational formulation for the coupled problem

We introduce the following constrained functional space:

$$K_{\mathbf{u}_\theta} = \left\{ \mathbf{u} \in H^1(\Omega \setminus \bar{B})^2,\ \mathbf{u} = 0 \text{ on } \partial\Omega \text{ and } \forall i\ \exists(\mathbf{v}_i, \omega_i) \in \mathbb{R}^2 \times \mathbb{R};\ \mathbf{u}(\mathbf{x}) = \mathbf{u}_{\theta_i} + \mathbf{v}_i + \omega_i \times (\mathbf{x} - \mathbf{x}_i) \text{ a.e. on } \partial B_i \right\}, \tag{7}$$

which is the space of functions defining a squirmer motion on ∂B, and we denote by K_0 the underlying vector space corresponding to $\mathbf{u}_{\theta_i} = \mathbf{0}$ for all i. Note that this is the space of functions defining a rigid motion on ∂B.

Let $(\mathbf{u}, p)$ be the solution of problem (2)-(3). On the one hand we write the incompressibility equation in its usual dual form. On the other hand we multiply the momentum equation in (2) by a test function $\widetilde{\mathbf{u}}$ in K_0 and integrate it by parts over $\Omega \setminus \bar{B}$. Using the boundary conditions of the problem as well as the balance of forces and angular momentum on each swimmer (3), we obtain the following variational formulation: we search the solution $(\mathbf{u}, p) \in K_{\mathbf{u}_\theta} \times L^2_0(\Omega \setminus \bar{B})$ such that

$$\left\{ \begin{array}{rcll} 2\mu \displaystyle\int_{\Omega\setminus\bar{B}} \mathbb{D}(\mathbf{u}) : \mathbb{D}(\widetilde{\mathbf{u}}) - \int_{\Omega\setminus\bar{B}} p\, \nabla\cdot\widetilde{\mathbf{u}} & = & 0, & \forall \widetilde{\mathbf{u}} \in K_0, \\ \displaystyle\int_{\Omega\setminus\bar{B}} q\, \nabla\cdot\mathbf{u} & = & 0, & \forall q \in L^2_0(\Omega\setminus\bar{B}), \end{array} \right. \tag{8}$$

where $L^2_0(\Omega \setminus \bar{B})$ stands for the set of L^2 functions over $\Omega \setminus \bar{B}$ with zero mean value.

We point out that each $\mathbf{u}_{\theta_i}$ being a regular function on the boundary of the particle ∂B_i, and satisfying $\int_{\partial B} \mathbf{u}_{\theta_i} \cdot \mathbf{n} = 0$, we can define a divergence-free function $\bar{\mathbf{u}}_\theta \in H^1(\Omega \setminus \bar{B})$ such that $\bar{\mathbf{u}}_\theta = \mathbf{u}_{\theta_i}$ a.e. in ∂B_i for all i, and $\bar{\mathbf{u}}_\theta = 0$ on $\partial\Omega$ (see for instance [9]). Thus, the functional space $K_{\mathbf{u}_\theta}$ can be written as $K_{\mathbf{u}_\theta} = \bar{\mathbf{u}}_\theta + K_0$, and thus problem (8) amounts to search the solution $\mathbf{u} = \bar{\mathbf{u}}_\theta + \bar{\mathbf{u}}$, where $\bar{\mathbf{u}} \in K_0$, and $p \in L^2_0(\Omega)$, such that

$$\left\{ \begin{array}{rcll} 2\mu \displaystyle\int_{\Omega} \mathbb{D}(\bar{\mathbf{u}}) : \mathbb{D}(\widetilde{\mathbf{u}}) - \int_{\Omega} p\, \nabla\cdot\widetilde{\mathbf{u}} & = & 2\mu \displaystyle\int_{\Omega} \mathbb{D}(\bar{\mathbf{u}}_\theta) : \mathbb{D}(\widetilde{\mathbf{u}}), & \forall \widetilde{\mathbf{u}} \in K_0, \\ \displaystyle\int_{\Omega} q\, \nabla\cdot\bar{\mathbf{u}} & = & 0, & \forall q \in L^2_0(\Omega), \end{array} \right. \tag{9}$$

By writing the problem in this form, it becomes straightforward that it has a unique solution in $K_{\mathbf{u}_\theta} \times L^2_0(\Omega\setminus\bar{B})$. In fact, K_0 is a closed subspace of $H^1(\Omega \setminus \bar{B})$ such that $H^1_0(\Omega \setminus \bar{B}) \subset K_0$, and the linear form in the right-hand side is continuous on $H^1(\Omega\setminus\bar{B})$, so that one can use classical results for the Stokes equations in mixed variational form (see for instance [3]) to prove the well-posedness of (9).

4. Fictitious domain approach

Different approaches have been used to simulate the motion of rigid and non-rigid bodies in a viscous fluid. One type of methods rely on meshing the fluid domain and computing the flow only in the fluid domain. Such methods require the use of complex meshes because of inclusions, and the redefinition of the mesh at each time step since the position of inclusions changes. Further computational techniques such as ALE-type mesh displacement can be used in order to optimize the mesh displacement procedure (see e.g. [15, 21, 25]). This

type of methods ensure a good accuracy in space because of the conforming character of the mesh, but their numerical cost can become extremely high because of dynamic mesh generation and the use of non-Cartesian meshes. Another approach relies on fictitious domain-type methods, which allow to use Cartesian grids in the whole domain. The rigid motion constraint can be taken into account by associating a Lagrange multiplier to its dual form (see e.g. [10, 11]), or it can be imposed by relaxing a term in the variational formulation, what in the case of rigid motion amounts to replace rigid zones by highly viscous ones (see [20, 31]).

In this work, we use a fictitious domain approach to deal with the constraint of squirming motion. This constraint can be enforced for each spherical inclusion using either a penalty method or a Lagrange multiplier.

4.1. **Penalty method to enforce the squirming motion constraint**

Let us define $\mathbf{u}_\theta$ as the solution of the Stokes equations inside each inclusion B_i such that it matches to the prescribed tangential velocity $\mathbf{u}_{\theta_i}$ of the swimmers on their boundary, that is:

$$\left\{\begin{array}{rcccl} -\mu\Delta\mathbf{u}_\theta + \nabla p_\theta &=& 0 & \text{in} & B, \\ \nabla\cdot\mathbf{u}_\theta &=& 0 & \text{in} & B, \\ \mathbf{u}_\theta &=& \mathbf{u}_{\theta_i} & \text{on} & \partial B_i, \quad \forall i\in\{1,...,N\}. \end{array}\right. \tag{10}$$

We slightly change the definition of the constrained functional space $K_{\mathbf{u}_\theta}$, which now involves functions defined on the whole domain Ω:

$$K_{\mathbf{u}_\theta} \;=\; \left\{\mathbf{u}\in H_0^1(\Omega)^2,\ \forall i\ \exists(\mathbf{v}_i,\omega_i)\in\mathbb{R}^2\times\mathbb{R};\ \mathbf{u}(\mathbf{x}) \;=\; \mathbf{u}_\theta \;+\; \mathbf{v}_i+\omega_i\times(\mathbf{x}-\mathbf{x}_i)\ \text{a.e. in}\ B_i\right\}\ .$$

$K_{\mathbf{u}_\theta}$ is the space of functions defining a squirmer motion in B, and we denote again by K_0 the underlying vector space corresponding to $\mathbf{u}_\theta=\mathbf{0}$ for all i and defining a rigid motion in B. Note that these spaces can also be written as follows [1]:

$$K_0=\left\{\mathbf{u}\in H_0^1(\Omega)^2,\ \mathbb{D}(\mathbf{u})=\mathbf{0}\ \text{a.e. in}\ B\right\} \tag{11}$$

and

$$K_{\mathbf{u}_\theta}=\left\{\mathbf{u}\in H_0^1(\Omega)^2,\ \mathbb{D}(\mathbf{u}-\mathbf{u}_\theta)=\mathbf{0}\ \text{a.e. in}\ B\right\}. \tag{12}$$

We rewrite the initial problem (8) as a minimization problem on the new constrained spaces : we search the solution $(\mathbf{u},p)\in K_{\mathbf{u}_\theta}\times L_0^2(\Omega)$ such that

$$\left\{\begin{array}{rcl} 2\mu\displaystyle\int_\Omega \mathbb{D}(\mathbf{u}):\mathbb{D}(\widetilde{\mathbf{u}}) - \int_\Omega p\,\nabla\cdot\widetilde{\mathbf{u}} &=& 0, \quad \forall\widetilde{\mathbf{u}}\in K_0, \\ \displaystyle\int_\Omega q\,\nabla\cdot\mathbf{u} &=& 0, \quad \forall q\in L_0^2(\Omega). \end{array}\right. \tag{13}$$

It can be shown that this variational problem has a solution $(\mathbf{u},p)\in K_{\mathbf{u}_\theta}\times L_0^2(\Omega)$ which is an extension of the unique solution of (8) to Ω such that $\mathbf{u}\in H_0^1(\Omega)$ and $\mathbf{u}(\mathbf{x})=\ \mathbf{u}_\theta+\mathbf{v}_i+\omega_i\times(\mathbf{x}-\mathbf{x}_i)$ a.e. in B. Note that this extension is unique for $\mathbf{u}$ but not for the pressure, since p is clearly underdetermined within the squirmer's bodies.

In order to relax the constraint of squirming motion on B in the functional space for velocity, we introduce the following penalty term in the variational formulation:

$$\frac{1}{\varepsilon}b(\mathbf{u}-\bar{\mathbf{u}}_\theta,\widetilde{\mathbf{u}}) \;=\; \frac{1}{\varepsilon}\int_B \mathbb{D}(\mathbf{u}-\mathbf{u}_\theta)\ :\ \mathbb{D}(\widetilde{\mathbf{u}})\,,$$

where b is the bilinear form $b(\mathbf{u},\widetilde{\mathbf{u}}):=\int_B\mathbb{D}(\mathbf{u}):\mathbb{D}(\widetilde{\mathbf{u}})$. When considering the minimization problem over a constrained domain associated to (13), this consists in relaxing the constraint by introducing the penalty term

$\frac{1}{2\varepsilon}\int_B |D(\mathbf{u}-\mathbf{u}_\theta)|^2$ in the minimized functional, so that $\mathbb{D}(\mathbf{u}-\mathbf{u}_\theta)$ goes to zero when ε goes to zero and $\mathbf{u}-\mathbf{u}_\theta$ tends to a rigid motion in B.

The variational formulation of the penalized problem is:

$$\left\{\begin{array}{rcll} 2\mu\displaystyle\int_\Omega \mathbb{D}(\mathbf{u}_\varepsilon) : \mathbb{D}(\widetilde{\mathbf{u}}) + \frac{1}{\varepsilon}\int_B \mathbb{D}(\mathbf{u}_\varepsilon-\mathbf{u}_\theta) : \mathbb{D}(\widetilde{\mathbf{u}}) - \int_\Omega p_\varepsilon \nabla\cdot\widetilde{\mathbf{u}} &=& 0\,, & \forall\widetilde{\mathbf{u}}\in H^1_0(\Omega), \\ \displaystyle\int_\Omega q\,\nabla\cdot\mathbf{u}_\varepsilon &=& 0, & \forall q\in L^2_0(\Omega), \end{array}\right. \tag{14}$$

We have $K_{\mathbf{u}_\theta} = \bar{\mathbf{u}}_\theta + \ker b$, where $b(\cdot,\cdot)$ is a symmetric, continuous and positive bilinear form on $H^1_0(\Omega)$. In addition we can write $b(\mathbf{u},\widetilde{\mathbf{u}}) = (B\mathbf{u}, B\widetilde{\mathbf{u}})$, with B the linear continuous operator that associates $\mathbf{u}\in H^1_0(\Omega)$ to the restriction of $\mathbb{D}(\mathbf{u})$ to B in $L^2(B)$. This operator having closed range, it can be proven that the penalty method converges linearly in ε (see [27]), *i.e.* the solution $\mathbf{u}_\varepsilon$ of problem (14) converges to the solution $\mathbf{u}$ of problem (13) as ε vanishes, and the convergence is of order 1 in ε. We refer again to [27] for a detailed analysis of a scalar version of this problem, which provides an error estimate for the space-discretized problem at the order $\varepsilon + h^{1/2}$ in the case a first-order method in space is used.

4.2. **Saddle-point formulation**

An alternative to the penalty method consists in writing the squirming constraint in dual form and considering a saddle-point formulation of the problem. For that purpose, we first extend the solution $(\mathbf{u},p)$ of (8) to the whole domain Ω so that it satisfies the Stokes equations inside the domain B. We modify again the constrained functional space $K_{\mathbf{u}_\theta}$, which will now be defined as follows:

$$K_{\mathbf{u}_\theta} \;=\; \left\{\mathbf{u}\in H^1_0(\Omega)^2,\ \forall i\ \exists(\mathbf{v}_i,\omega_i)\in\mathbb{R}^2\times\mathbb{R};\ \mathbf{u}(\mathbf{x}) \;=\; \mathbf{u}_{\theta_i} \;+\; \mathbf{v}_i + \omega_i\times(\mathbf{x}-\mathbf{x}_i) \text{ a.e. on } \partial B_i\right\}\ . \tag{15}$$

The underlying vector space corresponding to $\mathbf{u}_{\theta_i}=0$ for all i is again denoted by K_0. We search the solution $(\mathbf{u},p)\in K_{\mathbf{u}_\theta}\times L^2_0(\Omega)$ such that :

$$\left\{\begin{array}{rcll} 2\mu\displaystyle\int_\Omega \mathbb{D}(\mathbf{u}) : \mathbb{D}(\widetilde{\mathbf{u}}) - \int_\Omega p\,\nabla\cdot\widetilde{\mathbf{u}} &=& 0, & \forall\widetilde{\mathbf{u}}\in K_0, \\ \displaystyle\int_\Omega q\,\nabla\cdot\mathbf{u} &=& 0, & \forall q\in L^2_0(\Omega)\,. \end{array}\right. \tag{16}$$

Let us now denote by $\mathcal{R}_i$ the following operator,

$$\begin{array}{rccc} \mathcal{R}_i : & H^1_0(\Omega)^2 & \longrightarrow & L^2(\partial B_i)^2 \\ & \mathbf{v} & \mapsto & (\mathbf{v} - R_{B_i}(\mathbf{v}))_{|\partial B_i}\ , \end{array}$$

where $R_{B_i}(\mathbf{v})$ is the sum of the translation and the rotation given by the velocity field $\mathbf{v}$ on ∂B_i,

$$R_{B_i}(\mathbf{v}) = \frac{1}{|\partial B_i|}\int_{\partial B_i}\mathbf{v} \;+\; \frac{1}{R_i^2|\partial B_i|}\left(\int_{\partial B_i}\mathbf{r}\times\mathbf{v}\right)\times\mathbf{r}\ .$$

The squirming motion constraint can be written in the following dual form :

$$\mathbf{u}\in K_{\mathbf{u}_\theta} \iff \forall i\in\{1,\dots,N\},\ \int_{\partial B_i}\lambda\cdot\mathcal{R}_i(\mathbf{u}-\mathbf{u}_{\theta_i}) = 0 \quad \forall\lambda\in L^2(\partial B_i)^2\,, \tag{17}$$

and we consider a variational formulation of the associated saddle-point problem :

$$\left\{\begin{array}{rcl} 2\mu\displaystyle\int_\Omega \mathbb{D}(\mathbf{u}) : \mathbb{D}(\widetilde{\mathbf{u}}) - \int_\Omega p\,\nabla\cdot\widetilde{\mathbf{u}} - \sum_{i=1}^N \int_{\partial B_i} \lambda_i\cdot\mathcal{R}_i(\widetilde{\mathbf{u}}) &=& 0\,, \quad \forall\widetilde{\mathbf{u}}\in H^1_0(\Omega), \\ \displaystyle\int_\Omega q\,\nabla\cdot\mathbf{u} &=& 0, \quad \forall q\in L^2_0(\Omega) \\ \displaystyle\int_{\partial B_i}\widetilde{\lambda}_i\cdot\mathcal{R}_i(\mathbf{u}-\mathbf{u}_\theta) &=& 0, \quad \forall\widetilde{\lambda}_i\in(L^2(\partial B_i))^2\ ,\forall i\in\{1,\dots,N\}\ , \end{array}\right. \tag{18}$$

where $\lambda=(\lambda_i)_{i=1,\dots,N}\in\prod_{i=1}^N(L^2(\partial B_i))^2$ is the Lagrange multiplier associated to the squirmer constraint.

It can easily be shown (see for instance [1]) that if $(\mathbf{u},p,\lambda)\in H^1_0(\Omega)\times L^2_0(\Omega)\times\prod_{i=1}^N(L^2(\partial B_i))^2$ is a solution of the saddle-point problem (18), then $(\mathbf{u},p)$ is a solution of problem (16). The existence of the Lagrange multiplier λ does not result from standard theorem since $\mathcal{R}_i$ does not have closed range. But it can be proven in a constructive manner: let $(\mathbf{u}_0,p_0)$ be the unique solution of the initial problem (2)-(3) in $H^2(\Omega\setminus\bar{B})\times H^1(\Omega\setminus\bar{B})$ (see [33]). After an integration by parts of the first equation of (2) over $\Omega\setminus\bar{B}$ against a test function $\widetilde{\mathbf{u}}$ in the unconstrained space $H^1_0(\Omega)^2$, one has :

$$2\mu\int_{\Omega\setminus\bar{B}}\mathbb{D}(\mathbf{u}_0) : \mathbb{D}(\widetilde{\mathbf{u}}) - \int_{\Omega\setminus\bar{B}} p_0\,\nabla\cdot\widetilde{\mathbf{u}} = \sum_{i=1}^N\int_{\partial B_i}\sigma(\mathbf{u}_0)\cdot\mathbf{n}\cdot\widetilde{\mathbf{u}}\,.$$

Now using (3) we get the following equality :

$$\int_{\partial B_i}\sigma(\mathbf{u}_0)\cdot\mathbf{n}\cdot R_{B_i}(\widetilde{\mathbf{u}}) = 0, \quad \forall\widetilde{\mathbf{u}}\in H^1_0(\Omega)$$

and thus :

$$2\mu\int_{\Omega\setminus\bar{B}}\mathbb{D}(\mathbf{u}_0) : \mathbb{D}(\widetilde{\mathbf{u}}) - \int_{\Omega\setminus\bar{B}} p_0\,\nabla\cdot\widetilde{\mathbf{u}} = \sum_{i=1}^N\int_{\partial B_i}\sigma(\mathbf{u}_0)\cdot\mathbf{n}\cdot\mathcal{R}_i(\widetilde{\mathbf{u}})\ .$$

Recalling the notation of (4) and (5), we denote by $(\mathbf{u}_1,p_1)$ the solution of the following Stokes problem :

$$\left\{\begin{array}{rcll} -\mu\,\Delta\mathbf{u}_1+\nabla p_1 &=& 0 & \text{in } B, \\ \nabla\cdot\mathbf{u}_1 &=& 0 & \text{in } B, \\ \mathbf{u}_1 &=& \mathbf{u}_{\theta_i}+\mathbf{v}_i+\omega_i\times(\mathbf{x}-\mathbf{x}_i) & \text{on } \partial B_i,\ \forall i\in\{1,\dots,N\}. \end{array}\right.$$

This solution $(\mathbf{u}_1,p_1)$ is also in $(H^2(B))^2\times H^1(B)$. We denote by $\mathbf{u}_2$ the function whose restriction to $\Omega\setminus\bar{B}$ is $\mathbf{u}_0$ and the one to B is $\mathbf{u}_1$. The restriction of $\mathbf{u}_2$ to $\Omega\setminus\bar{B}$ and to B is in H^2, but $\mathbf{u}_2$ itself is only in $H^{3/2-\epsilon}(\Omega)$ (for some strictly positive ϵ), because of the jump of the normal derivatives on each ∂B_i. Nevertheless the following equality holds :

$$2\mu\int_B\mathbb{D}(\mathbf{u}_1) : \mathbb{D}(\widetilde{\mathbf{u}}) - \int_B p_1\,\nabla\cdot\widetilde{\mathbf{u}} = \sum_{i=1}^N\int_{\partial B_i}\sigma(\mathbf{u}_1)\cdot\mathbf{n}\cdot\mathcal{R}_i(\widetilde{\mathbf{u}})\ .$$

Hence, the sum of the last two equalities writes,

$$2\mu\int_\Omega\mathbb{D}(\mathbf{u}_2) : \mathbb{D}(\widetilde{\mathbf{u}}) - \int_\Omega p_2\,\nabla\cdot\widetilde{\mathbf{u}} = \sum_{i=1}^N\int_{\partial B_i}[\sigma(\mathbf{u}_2)\cdot\mathbf{n}]_{\partial B_i}\cdot\mathcal{R}_i(\widetilde{\mathbf{u}})\,,$$

where the symbol $[v]_{\partial B_i}$ denotes the jump of the quantity v across ∂B_i. Moreover, because $\mathbf{u}_2$ is divergence free and its trace on ∂B is equal to $\mathbf{u}_0$, the last two equalities of (18) are satisfied. This means that a solution of the saddle-point formulation is $\mathbf{u} = \mathbf{u}_2$, $p = p_2$ and $\lambda = \left([\sigma(\mathbf{u}_2)\cdot\mathbf{n}]_{\partial B_i}\right)_{i=1,\dots,N}$. Note that λ can be seen as a single layer force distribution which maintains the circular shape and ensures the prescribed tangential velocity.

5. Time discretization

We denote by $\Delta t > 0$ the time step and for any function $(\mathbf{x}, t) \to f(\mathbf{x}, t)$, we denote by f^n the approximation of $f(\cdot, n\Delta t)$. At $t = t^n = n\Delta t$, the solid domain is denoted by $B^n = \cup B_i^n$. For $i = 1...N$, the ith particle is defined by the position $\mathbf{x}_i^n$ of its center of gravity at time t^n, and its swimming direction θ_i^n.

Solving the fluid-structure interaction problem (2)-(3) at each time step we obtain the velocity field $\mathbf{u}$ on the whole domain, from which we can deduce the translational and angular velocity of each squirmer through (4) and (5). Note that in the case the penalty method is used to impose the squirmer motion, it is more convenient to use the following definition of the swimmers velocity, involving integrals on the surface of the particle :

$$\mathbf{v}_i^n = \frac{1}{|B_i|}\int_{B_i}(\mathbf{u}-\mathbf{u}_\theta), \tag{19}$$

$$\omega_i^n = \frac{1}{\displaystyle\int_{B_i}|\mathbf{x}-\mathbf{x}_i^n|^2}\int_{B_i}(\mathbf{x}-\mathbf{x}_i^n)\times(\mathbf{u}-\mathbf{u}_\theta). \tag{20}$$

The position and orientation of each squirmer at time t^{n+1} can then be updated by solving the ODEs (6) using for instance a first order explicit Euler method :

$$\mathbf{x}_i^{n+1} = \mathbf{x}_i^n + \Delta t\ \mathbf{v}_i^n\,, \qquad \theta_i^{n+1} = \theta_i^n + \Delta t\ \omega_i^n. \tag{21}$$

However, although contact is not supposed to happen when considering smooth particles in Stokes flow (see [8, 14]), this property is no more valid after time discretisation, and collisions between particles are likely to occur in numerical simulations. In fact, particles may overlap when their positions are updated after the velocity field computation, especially in the case of dense suspensions. Therefore possible numerical overlap must be prevented in order to guarantee robustness of the simulations. We use a numerical method proposed by Maury in [26], where inelastic collisions between rigid particles are computed. It consists of projecting the velocity field onto a set of admissible velocities, for which particles do not overcross in their next configuration.

Denoting by $\mathbf{X}^n := (\mathbf{x}_i^n)_{i=1,\dots,N}$ the position of the gravity centers of N particles at time t_n, the space of admissible velocities used is defined as follows :

$$K(\mathbf{X}^n) = \left\{\mathbf{V}\in\mathbb{R}^{2N},\ D_{ij}(\mathbf{X}^n) + \Delta t\,\mathbf{G}_{ij}(\mathbf{X}^n)\cdot\mathbf{V} \geq 0,\ \forall i<j\right\}, \tag{22}$$

where

$$D_{ij}(\mathbf{X}^n) = \left|\mathbf{x}_i^n - \mathbf{x}_j^n\right| - 2R_b$$

denotes the signed distance between two spheres B_i and B_j and

$$\mathbf{G}_{ij}(\mathbf{X}^n) = \nabla D_{ij} = (...,0,-\mathbf{e}_{ij},0,...,0,\mathbf{e}_{ij},0,...), \qquad \mathbf{e}_{ij} = \frac{\mathbf{x}_j-\mathbf{x}_i}{|\mathbf{x}_j-\mathbf{x}_i|}$$

is the gradient of the distance. Note that this space is a first order in time approximation of

$$E(\mathbf{X}^n) = \left\{\mathbf{V}\in\mathbb{R}^{2N},\ D_{ij}(\mathbf{X}^{n+1}) = D_{ij}(\mathbf{X}^n + \Delta t\,\mathbf{V}) \geq 0,\ \forall i<j\right\}, \tag{23}$$

and that in the case of spheres we have $K(\mathbf{X}^n) \subset E(\mathbf{X}^n)$.

The time algorithm reads as follows: in a first step, we solve the variational problem without taking into account the possible overlapping of the particles (thus defining an *a priori* velocity of the spheres), then compute the projection of this *a priori* velocity onto the set of admissible velocities defined by (22). This projection is performed by an Uzawa algorithm on its saddle-point formulation. We refer the reader to [5] for more details on this procedure of dealing with contacts in the framework of active suspensions.

6. Numerical results

6.1. **Space discretization and implementation**

We have implemented this algorithm with the finite element solver FreeFem++ (see [13]). The space discretization is carried out using the so-called mini-element (see [3]).

In the case the penalty approach is used to compute the velocity field in the whole domain, a reference solution $\hat{\mathbf{u}}_\theta$ is computed once on a reference sphere $\hat{B}$. It is then used at each time step in order to define the solution of (10) inside each squirmer, through translation and rotation operations on the reference solution $\hat{\mathbf{u}}_\theta$. The penality parameter ε in (14) has been taken equal to 10^{-3} in all the simulations, leading to an error on the constraint in L^2-norm (that is $err = \int_B (|\mathbb{D}(\mathbf{u} - \mathbf{u}_\theta)|^2)$ of approximatively 10^{-2}.

To solve the saddle point problem (18), the Uzawa algorithm is used. The Lagrange multipliers space is approximated by the space of P^1 function on a $1d$ mesh of the boundary of the swimmers. Therefore there are two different meshes: the mesh of the whole domain Ω on which the discrete velocity and pressure are defined, and the one for the Lagrange multipliers.

In order to compute accurately the fluid everywhere, we have chosen to keep at least one mesh element between two neighbouring particles (or between a particle and a wall). It simply consists in replacing $K(\mathbf{X}^n)$:

$$K(\mathbf{X}^n) = \left\{ \mathbf{V} \in \mathbb{R}^{2N},\ D_{ij}(\mathbf{X}^n) + \Delta t\, \mathbf{G}_{ij}(\mathbf{X}^n) \cdot \mathbf{V} \geq h,\ \forall i < j \right\},$$

where h denotes the maximum size of a mesh element.

6.2. **Single squirmer in a fluid at rest**

We show simulation results of a single neutral squirmer in a fluid at rest, two squirmers swimming close to each other in the same direction, and a squirmer swimming next to a wall. For these simulations we have used the penalty method, and we have prescribed biperiodic boundary conditions in the absence of walls, and no-slip conditions on walls.

Fig.2 shows on top the velocity field around a single squirmer in a unit square, and on the bottom the same velocity field computed in the frame of the squirmer. In the absence of any interaction, a squirmer swims straightforward with velocity $\frac{\alpha}{2}$.

Fig.3 shows the velocity field around a squirmer close to a wall. The presence of the wall affects the velocity of the squirmer. In fact, its angular velocity is not zero; the swimmer swims close to the wall for a while but at the same time it rotates outwards and then swims off. Fig.4 shows the velocity field around two squirmers close to each other. Similarly to the effect of a wall, the hydrodynamic interaction between two swimmers makes them rotate outwards, so that they swim off after a while. Note that in both cases there is no attraction effect at short time-scale : the distance between the squirmers (resp. the squirmer and the wall) does never decrease.

Further simulations have shown that neutral squirmers interact below a separation length of the order of the squirmer's diameter. Above this distance they do not affect each other's trajectory. These results concerning the short-range hydrodynamic interactions between swimmers, and between swimmers and walls, are of high importance for the understanding of the collective dynamics in concentrated suspensions.

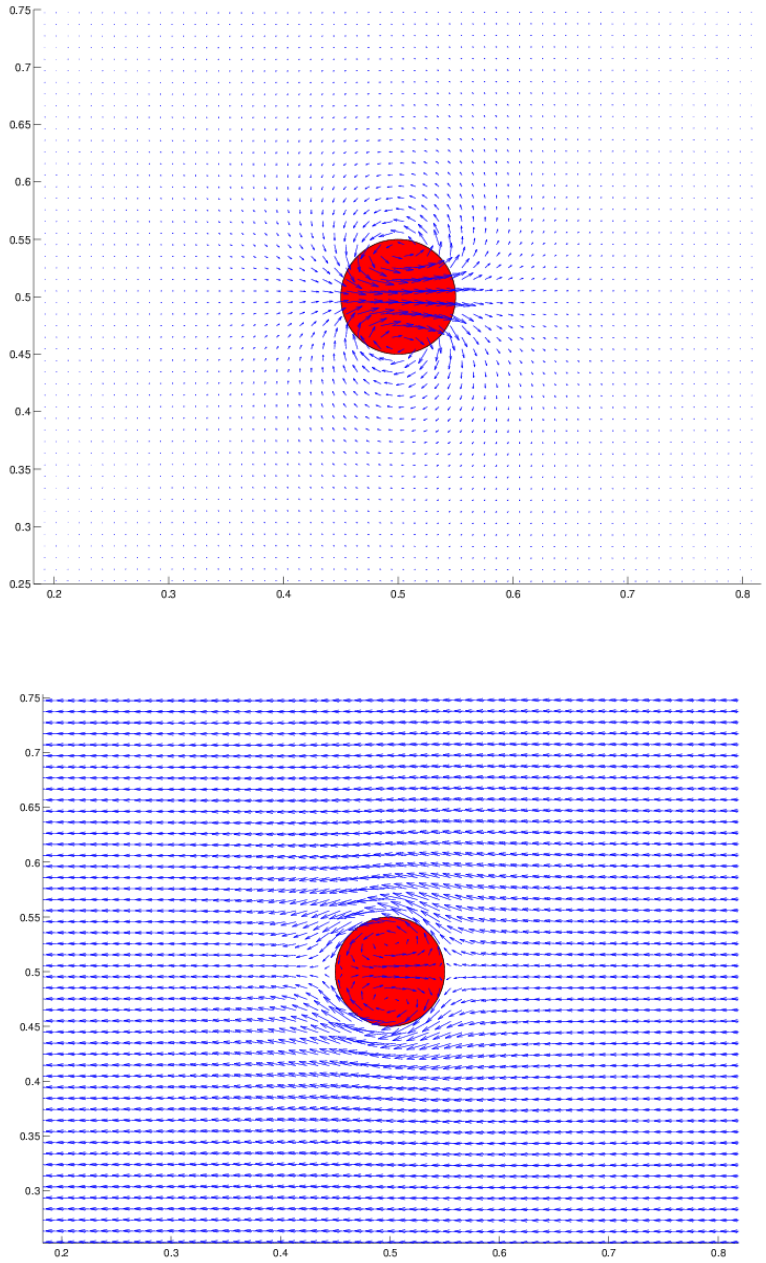

FIGURE 2. Velocity field produced by a single squirmer in the frame of the flow (top) and in the frame of the swimmer (bottom).

6.3. **Suspensions of squirmers in a flow with biperiodic conditions**

We have simulated the collective dynamics of dilute to dense squirmer suspensions, in a square domain with biperiodic boundary conditions. The problem has been solved using the penalty method.
Fig.5 shows the results obtained for a dilute suspension including 100 squirmers, what corresponds to a solid

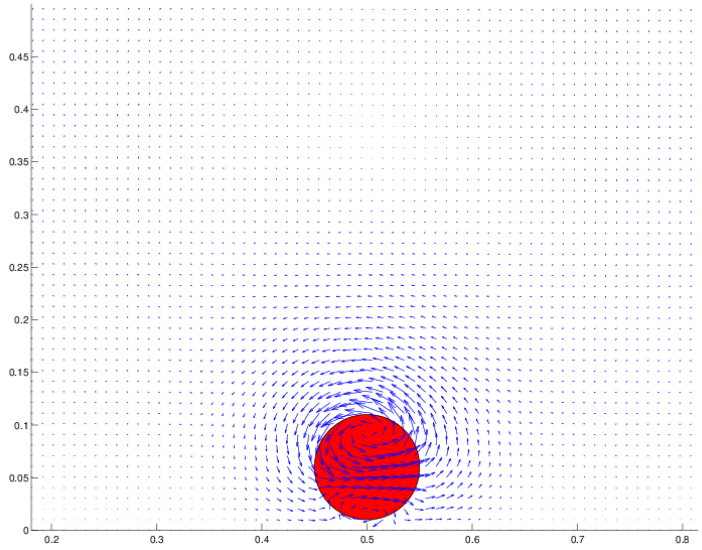

FIGURE 3. Velocity field produced by a single squirmer close to a wall

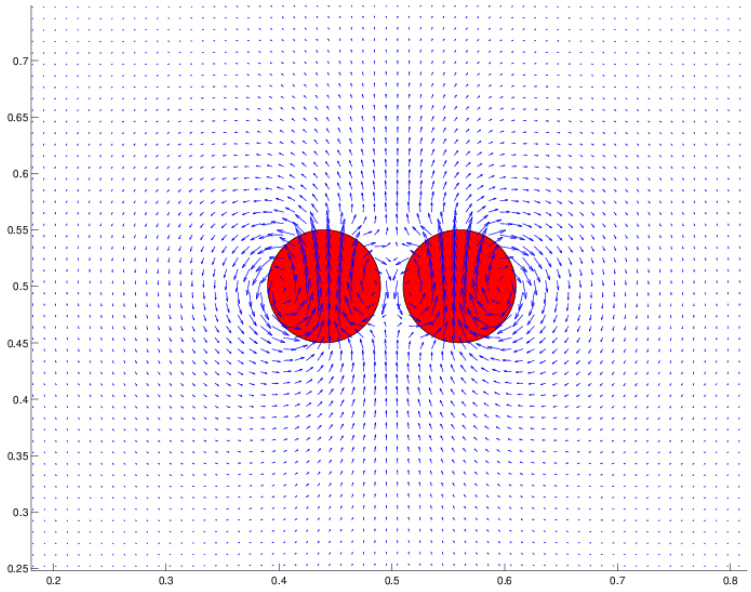

FIGURE 4. Velocity field produced by two squirmers swimming side by side

fraction of 12%. In this configuration, the swimmers essentially do not interact, except for some localized occurences in which they come close to each other. Thus their trajectories are almost straight and the initial swimming direction does not change significantly, as shown on the left in Fig.7.

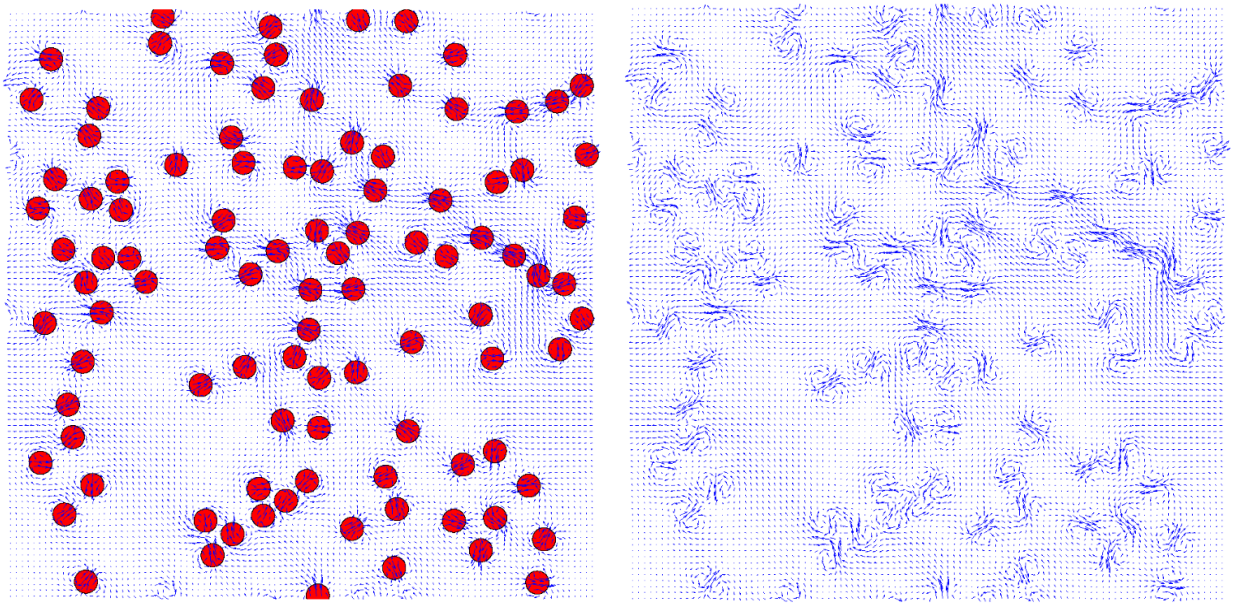

FIGURE 5. Dilute suspension of 100 squirmers in a flow at rest, at a given time step.

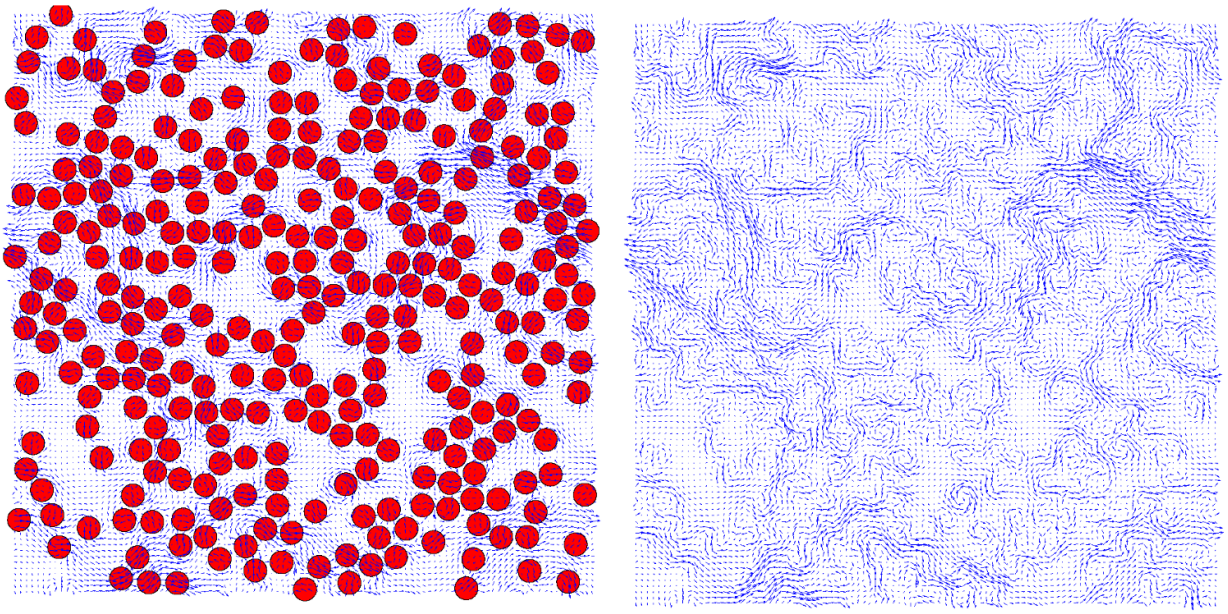

FIGURE 6. Dense suspension of 300 squirmers in a flow at rest, at a given time step.

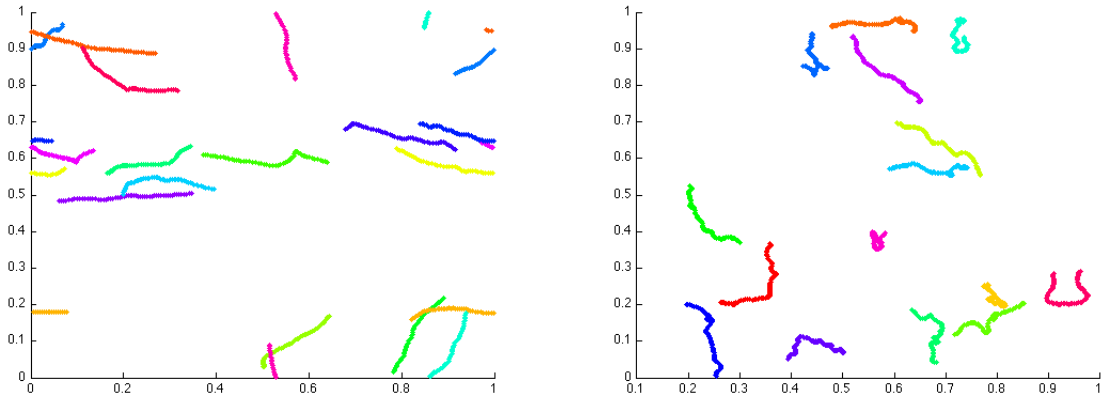

FIGURE 7. Trajectories of 15 squirmers in a dilute suspension (12%, left) and in a dense suspension (36%, right), during a simulation time of respectively 0.66 and 0.39 seconds.

Fig.6 shows the results obtained for a dense suspension including 300 squirmers, *i.e.* for a solid fraction of 36% : in this case the suspension is no more dilute and interactions between swimmers become significant. In fact one can see in Fig.7 that the trajectories of the swimmers are no more straight and their swimming direction changes significantly during the simulation. However, no other significant collective phenomenon is observed at this concentration, as for instance the emergence of coherent structures observed in suspensions of micro-swimmers imposing a force dipole on the fluid (see [5]). This might be due to the fact that interactions between neutral squirmers are relatively short-range. In fact, a neutral squirmer creates a perturbation of the velocity field in the fluid that decays as $\frac{1}{r^2}$ in two dimensions, whereas a dipole force creates a perturbation that decays more slowly as $\frac{1}{r}$.

6.4. **Effective viscosity of a suspension of squirmers**

The viscosity of a fluid can be measured thanks to a rheometer. In one of those experimental devices, the fluid is placed between two coaxial cylinders. When a given rotation is imposed to the inner cylinder, the fluid tends to drag the other cylinder. The viscosity is then deduced from the force that the fluid exerts on the outer cylinder. When considering a two-dimensional configuration, one can assume that the fluid is placed inbetween two horizontal plates at distance $2a$ from each other (see Fig.8). One plate moves at speed $S\boldsymbol{e}_x$ and the other one moves at speed $-S\boldsymbol{e}_x$, imposing a shear rate :

$$\dot{\gamma} = \frac{S}{a}.$$

One can then measure the shear stress, *i.e.* the average force applied by the fluid on the plates per surface unit in response to this shear :

$$F = \frac{\int_\Gamma (\sigma \cdot \mathbf{n}) \cdot \boldsymbol{\tau}}{2L},$$

where Γ denotes the surface of the two plates, L denotes the length of each plate, $\mathbf{n}$ is the normal vector Γ pointing outward and $\boldsymbol{\tau}$ is the tangential vector on Γ opposed to the shear flow. At time t, the apparent viscosity of the fluid is defined as the ratio of the shear stress to the shear rate:

$$\eta_{\text{app}}(t) = \frac{F}{\dot{\gamma}}.$$

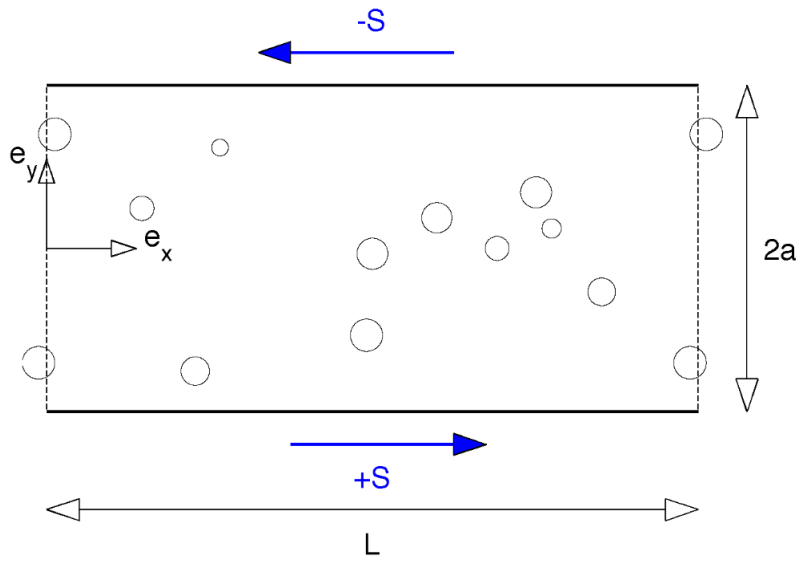

FIGURE 8. Schematic view of a rheometer in two dimensions.

In the case of a suspension, the apparent viscosity is likely to vary with time, depending on the instantaneous configuration of the particles. Therefore one usually considers the effective viscosity :

$$\eta_{\text{eff}} = \lim_{T \mapsto +\infty} \frac{1}{T} \int_0^T \eta_{\text{app}}(t) \mathrm{d}t.$$

In the case of active suspensions, the measurement or computation of the effective viscosity is particularly interesting, since different phenomena can arise depending on the type of motion. Elongated pusher-like swimmers, for instance, tend to decrease the effective viscosity, while elongated puller-like swimmers tend to increase it (see for instance [12] for an asymptotic analysis, and [32] and [30] for an experimental study of this phenomenon). On the contrary, spherical pusher- or puller-like swimmers do not modify the effective viscosity in suspensions as shown by Berlyand and coauthors in [12] in the dilute and semi-dilute regimes, and observed through numerical simulations by Ishikawa and Pedley in [18].

We have computed the effective viscosity in suspensions of squirmers through simulations of the model presented in section 2. The computational domain considered is a square of side 1, discretized using 350 nodes on each side, and the radius R_b of the squirmers has been taken equal to 0.015, what corresponds to an average of 10 mesh-cells on the length of a single particle. Shear is imposed through non homogenous Dirichlet conditions $u_y = 0$ and $u_x = \pm S$, with $S = 0.5$, on the upper and lower walls. The domain is periodic in the x-direction. Three suspensions of squirmers have been considered, with solid fractions of about 10%, 20% and 30%, and containing respectively 150, 300 and 450 squirmers. The individual swimming velocity of a squirmer in a fluid at rest is given by $\frac{\alpha}{2}$, where α is the proportionality constant in the prescribed tangential velocity $\mathbf{u}_\theta$ (1). The shear flow in presence of squirmers can therefore be characterized by the non-dimensional quantity:

$$\Phi = \frac{2\dot{\gamma} R_b}{\alpha}. \tag{24}$$

We present simulations performed in the regime where $\Phi = 0.06$, *i.e.* in the regime where the shear only slightly perturbs the motion of the swimmers. Fig.9, Fig.10 and Fig.11 show the evolution of the apparent viscosity

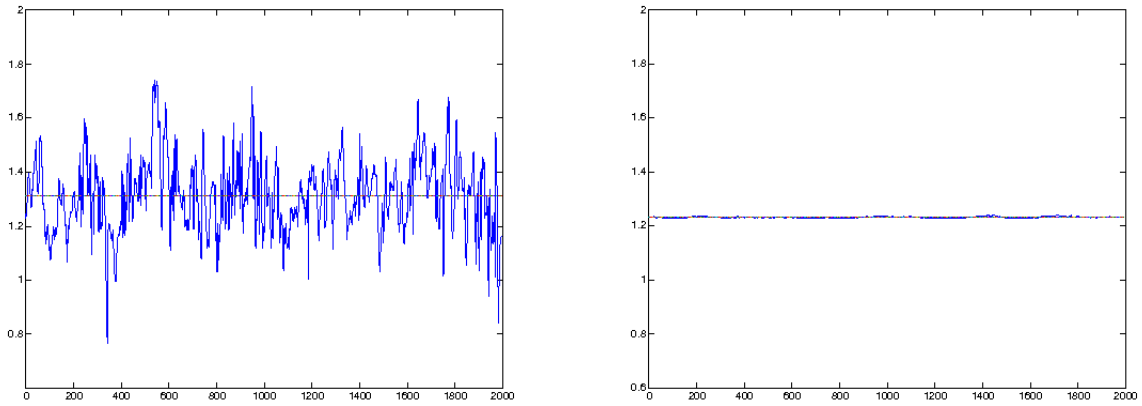

FIGURE 9. Apparent viscosity η_{app}/η_0 with respect to time of a dilute suspension (concentration 10%) of squirmers (left) and passive particles of same size (right). The horizontal line represents the effective viscosity.

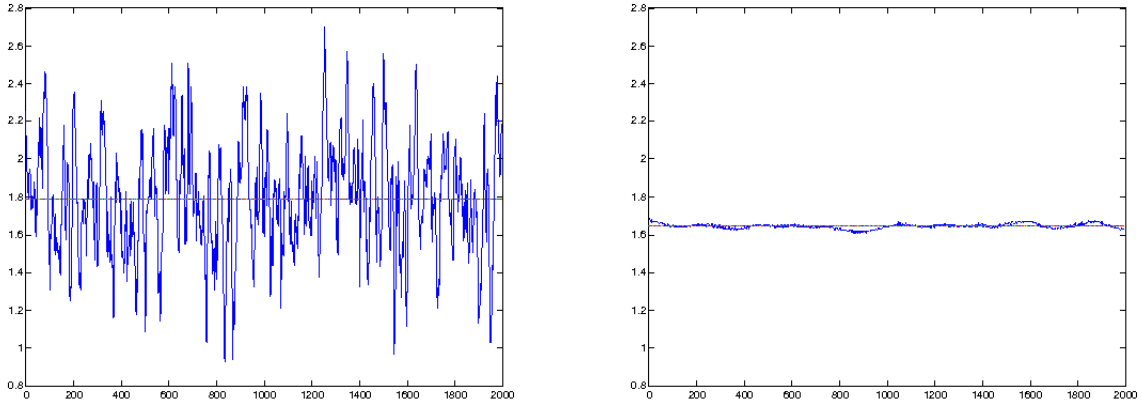

FIGURE 10. Apparent viscosity η_{app}/η_0 with respect to time of a 20% concentrated suspension of squirmers (left) and passive particles of same size (right). The horizontal line represents the effective viscosity.

$\frac{\eta_{app}}{\eta_0}$, where η_0 is the viscosity of the ambient fluid. Each squirmer suspension is compared to the corresponding passive suspension, that means a suspension of same-sized passive particles at the same concentration. The effective viscosity, represented by the horizontal line, is computed as the average of the apparent viscosity over the whole simulation.

In this regime and at the concentrations considered, we observe that the effective viscosity is slightly higher for the active suspension than for the corresponding passive suspension. Denoting by η_{eff} the effective viscosity of the active suspension, and by $\eta_{\tilde{eff}}$ the effective viscosity of the corresponding passive suspension, we have a relative effective viscosity

$$\frac{\eta_{eff} - \eta_{\tilde{eff}}}{\eta_{\tilde{eff}}}$$

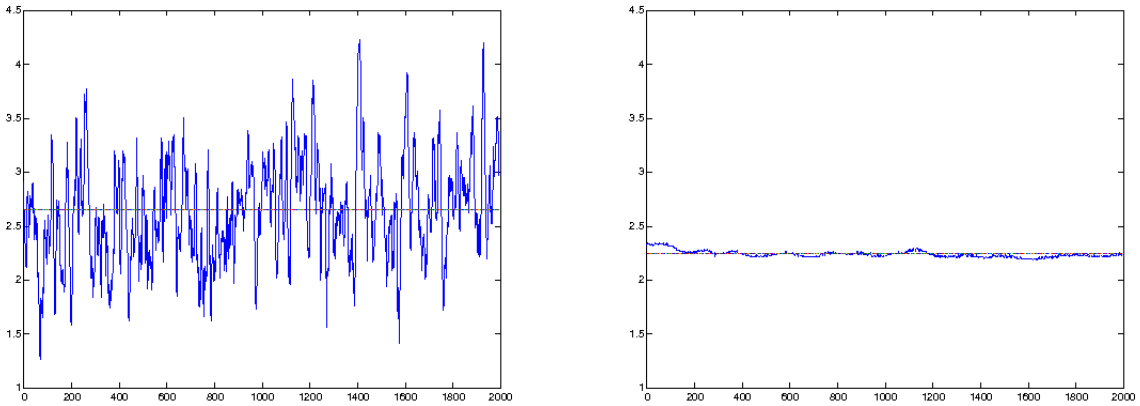

FIGURE 11. Apparent viscosity η_{app}/η_0 with respect to time of a 30% concentrated suspension of squirmers (left) and passive particles of same size (right). The horizontal line represents the effective viscosity.

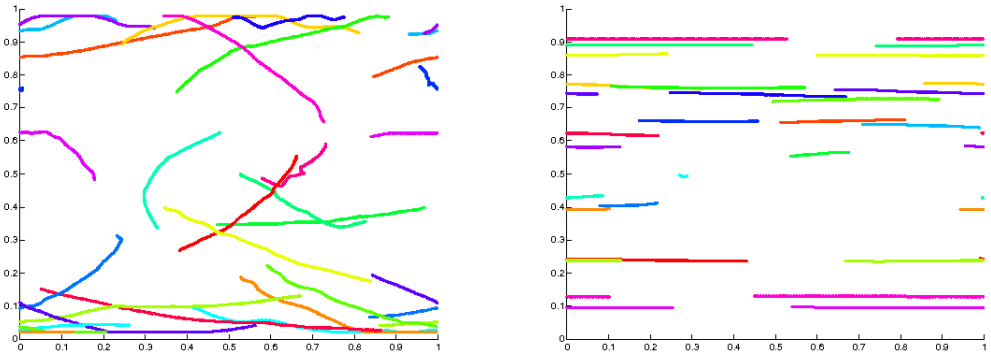

FIGURE 12. Trajectories of some squirmers in the 10% suspension.

of less than 10% for the suspensions with 10% and 20% solid fraction, and about 20% for the suspension with a solid fraction of 30%. In the case of pusher- or puller-like swimmers (see for instance [12]) the effective viscosity of the suspension can be drastically modified by the motility of the particles beyond the dilute regime limit. Neutral-squirmer-model swimmers affect only slightly the rheological properties of the fluid in the presented simulations; and further numerical simulations should be performed with higher swimmer concentrations and different values of Φ.

Let us note however that the dynamics in the sheared active suspensions are very different from the corresponding passive suspensions. On one hand the amplitude of variation of the apparent viscosity is far more important. On the other hand, in the case of passive suspensions, the particles just follow the shear flow, whereas in the active suspensions their trajectories are much more independent of the shear flow, as can be seen on Fig.12, where the trajectories of some squirmers in the 10% suspension are displayed over a simulation time of 8 seconds.

7. Conclusion

To model the individual and collective motion of neutral squirmer up to high concentrations, we performed numerical simulations based on a fictitious domain approach. We found that two initially parallel squirmers turn outwards and move away from each other. The same behavior was found in the case of a swimmer swimming parallel to a wall. Simulations of dilute and concentrated suspensions of neutral squirmers have shown that unlike pushers and pullers, neutral squirmers do not give rise to coherent structures as vortices or jets, and that they slightly affect the rheological properties of the suspension with respect to the case of passive spherical particles of the same size. In fact, for a packing fraction of 30%, the viscosity of the active suspension is about 20% higher than the one for the passive suspension. It would be interesting to measure this difference experimentally in suspensions of self-propelled droplets, but also challenging, given the usual precision of such measurements [30, 32]. However, it is not clear whether self-propelled droplets behave like neutral squirmers, or if they apply a dipole force on the fluid. The numerical model presented here may help to clarify that. Therefore, as a next step, we would like to add an active stresslet to the squirmer slip velocity (see for instance [24]), and see how this affects the collective dynamics of these model-swimmers.

References

[1] G. Allaire. Numerical analysis and optimization. In *An Introduction to Mathematical Modelling and Numerical Simulation*. Oxford University Press, 2007.

[2] J.R. Blake. A spherical envelope approach to ciliary propulsion. *J. Fluid Mech.*, 46:199–208, 1971.

[3] F. Brezzi and M. Fortin. Mixed and hybrid finite element methods. In *Springer Series in Computational Mathematics. Vol. 15*. Springer-Verlag, 1991.

[4] L.H. Cisneros, J.O. Kessler, S. Ganguly, and R.E. Goldstein. Dynamics of swimming bacteria: transition to directional order at high concentration. *Phys. Rev. E*, 83:061907, 2011.

[5] A. Decoene, S. Martin, and B. Maury. Microscopic modelling of active bacterial suspensions. *Mathematical Modelling of Natural Phenomena*, pages 98–129, 2011.

[6] M.T. Downton and H. Stark. Simulation of a model microswimmer. *J. Phys.: Condens. Matter*, 21:204101, 2009.

[7] K. Dresher, K.C. Leptos, I. Tuval, T. Ishikawa, T. Pedley, and R.E. Goldstein. Dancing *Volvox*: hydrodynamic bound states of swimming algae. *Phys. Rev. Lett.*, 102:168101, 2009.

[8] D. Gérard-Varet and M. Hillairet. Regularity issues in the problem of fluid structure interaction. *Arch. Rat. Mech. Anal.*, 19:375–407, 2010.

[9] V. Girault and P. A. Raviart. Finite element methods for the Navier-Stokes equations. theory and algorithms. Springer-Verlag, 1986.

[10] R. Glowinski. Finite element methods for incompressible viscous flow. In P.G. Ciarlet and J.-L. Lions, editors, *Handbook of Numerical Analysis, Vol. IX*. Ed. North-Holland,, 2003.

[11] R. Glowinski, T.W. Pan, T.I. Hesla, D.D. Joseph, and J. Périaux. A fictitious domain approach to the direct numerical simulation of incompressible viscous flow past moving rigid bodies: application to particulate flow. *J. Comp. Phys.*, 169:363–427, 2001.

[12] B.M. Haines, I.S. Aranson, L. Berlyand, and D.A. Karpeev. Effective viscosity of bacterial suspensions: A three-dimensional pde model with stochastic torque. *Comm. Pure Appl. Anal.*, pages 19–46, 2012.

[13] F. Hecht, O. Pironneau, A. le Hyaric, and K. Ohtsuka. Freefem++, finite elements software. http://www.freefem.org/ff++/, 2011.

[14] M. Hillairet. Lack of collision between solid bodies in a 2d constant-density incompressible flow. *Commun. Part. Diff. Eq.*, 32:1345–1371, 2007.

[15] H.H. Hu. Direct simulation of flows of solid-liquid mixtures. *Int. J. Multiphase Flow*, 22(2):335–352, 1996.

[16] T. Ishikawa, Simmonds M.P., and T.J. Pedley. Hydrodynamic interaction of two swimming model micro-organisms. *J. Fluid Mech.*, 568:119–160, 2006.

[17] T. Ishikawa and T.J. Pedley. Diffusion of swimming model mirco-organisms in a semi-dilute suspension. *J. Fluid Mech.*, 588:437, 2007.

[18] T. Ishikawa and T.J. Pedley. The rheology of semi-dilute suspensions of swimming micro-organisms. *J. Fluid Mech.*, 588:399–435, 2007.

[19] T. Ishikawa, N. Yoshida, H. Ueno, M. Wiedeman, Y. Imai, and T. Yamaguchi. Energy transport in a concentrated suspension of bacteria. *Phys. Rev. Lett.*, 107:028102, 2011.

[20] J. Janela, A. Lefebvre, and B. Maury. A penaly method for the simulation of fluid-rigid body interaction. *ESAIM: Proc.*, 14:115–123, 2005.

[21] A. Johnson and T.E. Tezduyar. Simulation of multiple spheres falling in a liquid-filled tube. *Comput. Method. Appl. M.*, 134(3):351–373, 1996.
[22] D. L. Koch and G. Subramanian. Collective hydrodynamics of swimming microorganisms: living fluids. *Annu. Rev. Fluid Mech.*, 43:637–659, 2011.
[23] M.J. Lighthill. An adaptative augmented Lagrangian method for three-dimensional multimaterial flows. *Commum. Pure Appl. Math.*, 5:109–118, 1952.
[24] I. Llopis and I. Pagonabarraga. Hydrodynamic interactions in squirmer motion: swimming with a neighbour and close to a wall. *J. Non-Newtonian Fluid Mech.*, 165:946–952, 2010.
[25] B. Maury. Direct simulations of 2D fluid-particle flows in biperiodic domains. *J. Comput. Phys.*, 156:325–351, 1999.
[26] B. Maury. A time-stepping scheme for inelastic collisions. *Numer. Math.*, 102(4):649–679, 2006.
[27] B. Maury. Numerical analysis of a finite element / volume penalty method. *SIAM J. Numer. Anal.*, 47(2):1126–1148, 2009.
[28] S. Michelin and E. Lauga. Efficiency optimization and symmetry-breaking in a model of ciliary locomotion. *Phys. Fluids*, 22:111901, 2010.
[29] E. M. Purcell. Life at low reynolds number. *American Journal of Physics*, pages 3–11, 1977.
[30] S. Rafai, L. Jibuti, and P. Peyla. Effective viscosity of microswimmer suspensions. *Phys. Rev. Lett.*, 2010.
[31] T.N. Randrianarivelo, G. Pianet, S. Vincent, and J.P. Caltagirone. Numerical modelling of solid particle motion using a new penalty method. *Int. J. Numer. Meth. Fluids*, 47:1245–1251, 2005.
[32] A. Sokolov and I.S. Aranson. Reduction of viscosity in suspension of swimming bacteria. *Phys. Rev. Lett.*, 103:148101, 2009.
[33] T. Takahashi. Analysis of strong solutions for the equations modeling the motion of a rigid-fluid system in a bounded domain. *Adv. Differential Equations*, 8:1499–1532, 2003.
[34] S. Thutupalli, R. Seemann, and S. Herminghaus. Diffusion of swimming model mirco-organisms in a semi-dilute suspension. *New Journal of Physics*, 13, 2011.